JGR Atmospheres

RESEARCH ARTICLE
10.1029/2023JD038843

Triple-Dip La Niñas in 1998–2001 and 2020–2023: Impact of Mean State Changes

Xiaofan Li[1,2], Zeng-Zhen Hu[3], Michael J. McPhaden[4], Congwen Zhu[5], and Yunyun Liu[6]

[1]Key Laboratory of Geoscience Big Data and Deep Resource of Zhejiang Province, School of Earth Sciences, Zhejiang University, Hangzhou, China, [2]Southern Marine Science and Engineering Guangdong Laboratory (Zhuhai), Zhuhai, China, [3]Climate Prediction Center, NCEP/NWS/NOAA, College Park, MD, USA, [4]NOAA/Pacific Marine Environment Laboratory, Seattle, WA, USA, [5]State Key Laboratory of Severe Weather, Chinese Academy of Meteorological Sciences, Beijing, China, [6]CMA Climate Study Key Laboratory, National Climate Center, China Meteorological Administration, Beijing, China

Key Points:

- The physical processes responsible for the evolution of the 1998–2001 and 2020–2023 triple-dip La Niñas were different
- Ocean heat content as a precursor was more important for the predictability of the 1998–2001 La Niña than the 2020–2023 La Niña
- Stronger surface easterlies and zonal sea surface temperature gradient in the equatorial Pacific contributed to the predictability of the 2020–2023 La Niña

Supporting Information:

Supporting Information may be found in the online version of this article.

Correspondence to:

Z.-Z. Hu,
Zeng-Zhen.Hu@noaa.gov

Citation:

Li, X., Hu, Z.-Z., McPhaden, M. J., Zhu, C., & Liu, Y. (2023). Triple-dip La Niñas in 1998–2001 and 2020–2023: Impact of mean state changes. *Journal of Geophysical Research: Atmospheres*, *128*, e2023JD038843. https://doi.org/10.1029/2023JD038843

Received 8 MAR 2023
Accepted 20 AUG 2023

Abstract This study compares the evolution of atmospheric and oceanic anomalies as well as predictions for the two most recent triple-dip La Niña events in 1998–2001 and 2020–2023. Subsurface cooling in the equatorial Pacific was stronger and more persistent during 1998–2001. In contrast, surface easterly winds were stronger during 2020–2023 as was the east-west sea surface temperature (SST) contrast along the equator. We argue that in the absence of appreciable equatorial Pacific heat discharge, persistent and strong surface trade winds and a strengthened mean zonal SST contrast across the tropical Pacific contributed to the development of the 2020–2023 triple-dip La Niña. In terms of the subsurface layer heat budget, the growth and maintenance of unusually cold SSTs during the triple-dip La Niña in 1998–2001 were mainly the result of ocean vertical entrainment and diffusion, as well as meridional advection, associated with enhanced equatorial upwelling; while for the triple-dip La Niña in 2020–2023, zonal advection was the largest contributor. The two events were mostly well predicted by multi-model averages at 1–8 months lead times. We hypothesize that mean state change with enhanced zonal SST contrast and trade winds over the last several decades altered the physical processes associated with the growth and maintenance of the most recent La Niña, affecting its predictability. Successful prediction in real-time of the 2020–2023 event more than half a year in advance was surprising because there was little memory in oceanic heat content which is often considered a key predictor.

Plain Language Summary El Niño-Southern Oscillation is the strongest interannual variability on Earth and the main source of global seasonal climate predictability. Here, we examine the evolution of oceanic and atmospheric anomalies in the tropical Pacific during two triple-dip La Niñas in 1998–2001 and 2020–2023, comparing the physical processes that gave rise to them and the skill in predicting them. Our results show that the processes giving rise to these events were different and likely affected by mean state changes in the tropical Pacific. In particular, the easterly trade winds and zonal SST contrast across the basin have strengthened that played a crucial role in the growth, maintenance, and prediction of the La Niña in 2020–2023. The evolution of the La Niña in 2020–2023 was successfully predicted in real-time more than half a year in advance, which is surprising because there was little memory in oceanic heat content which is often considered a key predictor.

1. Introduction

El Niño-Southern Oscillation (ENSO) plays a crucial role in seasonal-interannual climate variability and predictability (National Research Council, 2010). Since the pioneering work of Bjerknes (1969), the impacts of ENSO on global and regional climate have been well documented (Li, Hu, Liang, & Zhu 2019; Li et al., 2023; McPhaden et al., 2020; Yulaeva & Wallace, 1994). Coupled ocean-atmosphere interactions in the Pacific provide the scientific foundation for operational seasonal-to-interannual climate forecasts (e.g., O'Lenic et al., 2008; Peng et al., 2013). However, ENSO is irregular and diverse in its properties because of noise and nonlinearity in the system (An et al., 2020; Capotondi et al., 2015; Timmermann et al., 2018) which makes it challenging to accurately predict ENSO and its global impacts (McPhaden et al., 2015). For example, predictions of 2010–2011 La Niña (e.g., R.-H. Zhang et al., 2013), 2014–2015 El Niño (e.g., Zhu et al., 2016), and 2017–2018 La Niña were unsuccessful for the majority of ENSO prediction models (https://iri.columbia.edu/our-expertise/climate/enso/; Huang et al., 2017; Z.-Z. Hu et al., 2020). Thus, further understanding ENSO dynamics is very important, particularly for rare but highly consequential multi-year La Niña events (McPhaden, 2023).

Appreciable irregularity of the ENSO cycle between its cold and warm phases leads to asymmetric evolution in which El Niño normally lasts about 1 year from boreal summer to the following spring, while La Niña often persists over two and in some cases three consecutive years (DiNezio et al., 2017; Z.-Z. Hu et al., 2014; Kim & Yu, 2022; Ohba & Ueda, 2009; Okumura et al., 2011; Song et al., 2022). According to the Climate Prediction Center (CPC) Oceanic Niño Index definition for ENSO, among the total of 20 El Niño events during 1951–2023 (Figure S1 in Supporting Information S1), 15 (75%) were 1-year duration and 5 (25%) persisted for 2 years. Among a total of 13 La Niña events, 4 (31%) were 1 year, 6 (46%) lasted 2 years (double-dip events), and 3 (23%) persisted for 3 years (triple-dip events) (Z. Gao et al., 2023). This asymmetry in multi-year El Niño and La Niña events represents a deviation from a pure cyclic behavior of ENSO, which can not be fully explained by the original recharge oscillator theory (Z.-Z. Hu et al., 2017; Jin, 1997; Kessler, 2002; Yu & Fang, 2018). A variety of processes may account for these asymmetries between El Niño and La Niña, including a nonlinear atmospheric response to SST (e.g., Ohba & Ueda, 2009), the contrasting influence of the Indian Ocean on the decay phases of El Niño and La Niña (e.g., Okumura et al., 2011), and the asymmetry associated with the recharge and discharge dynamics (Z.-Z. Hu et al., 2017) linked to nonlinear oceanic dynamical processes (DiNezio & Deser, 2014; Hayashi & Jin, 2017; Z.-Z. Hu et al., 2014; Song et al., 2022).

Considering the asymmetry in event duration, the occurrence of triple-dip La Niñas is particularly striking. Since 1951, three triple-dip La Niña events (1973–1976, 1998–2001, 2020–2023) have occurred. The first two events developed in the wake of strong El Niños in 1972–1973 and 1997–1998 (McPhaden, 1999), respectively, while in contrast, the latest event occurred after a borderline El Niño in 2019–2020 (Figure 1a; C. Gao et al., 2022; Hasan et al., 2022; Huang et al., 2022; Li et al., 2022; R.-H. Zhang et al., 2022). Among the six multi-year La Niña events since 1982 (Figure S2 in Supporting Information S1), two of them lasted into a third year (1998–2001 and 2020–2023; Figure 1), while the other four were followed by either El Niños (2009–2010 and 2018–2019), or neutral conditions (1985–1986 and 2012–2013).

Given the rarity of triple-dip La Niña events, their evolution and prediction skill have not been well documented. Thus, our purpose is to compare the evolution as well as the prediction of the two most recent events, and to examine the associated physical processes involved in their variability and predictability. Due to data availability, we have restricted our focus to the 1998–2001 and 2020–2023 events since they are the best documented. We will examine similarities and differences in oceanic and atmospheric anomalies, such as sea surface temperature (SST), subsurface ocean temperature, atmospheric deep convection, and low-level wind anomalies in the tropical Pacific. Furthermore, the impact of the mean state change on the growth and maintenance of triple-dip La Niña events will be addressed. Lastly, the hindcasts of the 1998–2001 event and real-time predictions of the 2020–2023 event will be verified.

The rest of the paper is organized as follows. The observational and model prediction data are introduced in Section 2. Sections 3–5 show the similarities and differences in the evolution of oceanic and atmospheric anomalies in the equatorial Pacific during the 2020–2023 and 1998–2001 La Niñas, the impact of the tropical Pacific mean state changes, and the hindcasts and real-time predictions of the two triple-dip La Niñas, respectively. We conclude with a summary and discussion in Section 6.

2. Observational and Model Prediction Data

For observations, we use the Global Ocean Data Assimilation System (GODAS) which is a real-time ocean reanalysis (Behringer & Xue, 2004) that has long been used for monitoring the global ocean and ENSO evolution at CPC (Z.-Z. Hu et al., 2022). The reanalysis is based on a quasi-global configuration of the Geophysical Fluid Dynamics Laboratory Modular Ocean Model version 3 (GFDL MOMv3) with a domain from 75°S to 65°N. Both temperature and synthetic salinity profiles are assimilated in a 3-Dimensional Variational Analysis (3DVA) scheme with 40 vertical levels and a horizontal resolution of 1° by 1°, enhanced to 1/3° in the meridional direction within 10° of the equator. The GODAS is forced by the momentum flux, heat flux, and freshwater flux from the National Centers for Environmental Prediction and the Department of Energy reanalysis (NCEP/DOE; Kanamitsu et al., 2002).

Recharge/discharge processes exchange heat between the equatorial band and adjacent off-equatorial areas to the north and south (Jin, 1997). An index for this heat exchange is given by the warm water volume which is defined as the GODAS monthly mean 20°C isotherm depth (D20) anomaly averaged in (5°S–5°N, 120°E–80°W; Meinen

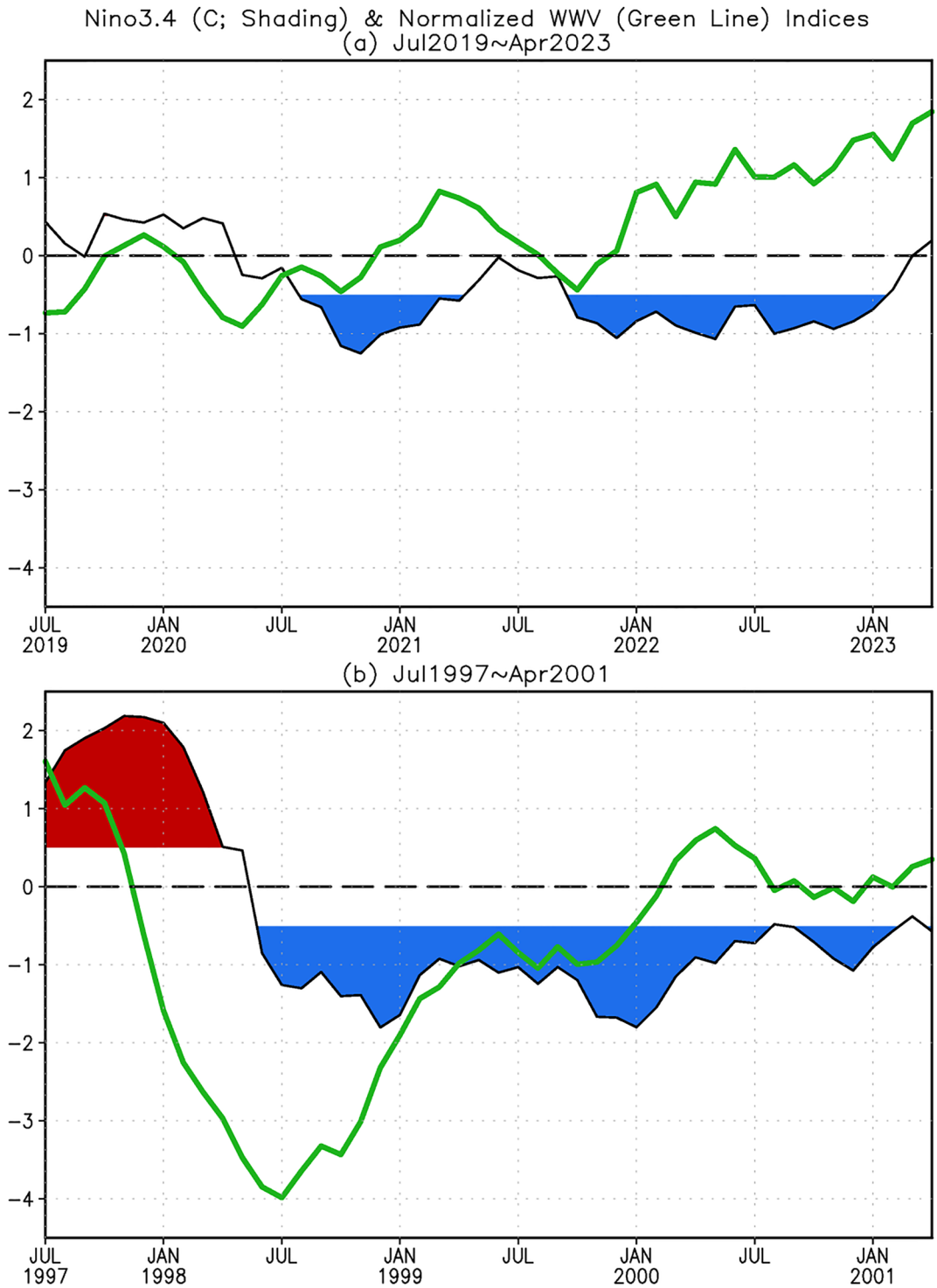

Figure 1. Monthly mean of the Niño3.4 (black line; °C) and normalized warm water volume (WWV) (green line) indices during (a) July 2019 to April 2023 and (b) July 1997 to April 2001. WWV is normalized by its standard deviation over January 1991 to December 2020, which is 6.4 m. The Niño3.4 index is shaded with a value larger than 0.5°C or smaller than −0.5°C.

& McPhaden, 2000). We also analyze the heat budget in the ocean mixed layer (Z.-Z. Hu et al., 2016; Huang et al., 2010):

$$\frac{\partial T}{\partial t} = Q_u + Q_v + Q_w + Q_{zz} + Q_q + R$$

where, $\partial T/\partial t$ is the temperature tendency, Q_u and Q_v are zonal and meridional advection, respectively; and Q_w (Q_{zz}) represents vertical entrainment (diffusion). Q_q is adjusted surface heat flux, which is the net surface heat flux plus a correction for penetrative shortwave radiation lost below the base of the mixed layer. R represents the effects of horizontal heat diffusion, sub-monthly processes, and imbalances in the heat budget due to the GODAS data assimilation process (see below).

The ocean mixed-layer heat budget is computed with pentad data in the global ocean from 74°S to 64°N on a 1° × 1° resolution from GODAS. The mixed layer depth (MLD) was determined with the criterion of a density difference of 0.125 kg m^{-3} between the surface and the bottom of the mixed layer. The MLD is calculated using the pentad fields of temperature and salinity from GODAS. Using GODAS output from 1979 to 2008, Huang et al. (2010) verified that the heat budget overall captures the physical processes controlling SST variability associated with ENSO. The GODAS data assimilation method introduces sources and sinks of heat such that the mixed layer heat balance does not exactly close. In most situations though, the imbalance is relatively small and does not adversely affect the interpretation of dominant physical processes affecting the mixed layer heat budget.

Monthly mean SSTs are from the upgraded version of Optimum Interpolation OIv2.1 with improved bias corrections (Huang et al., 2021). OIv2.1 SSTs are a blend of in situ ship and buoy SSTs with satellite SSTs derived from the Advanced Very High-Resolution Radiometer. OIv2.1 data are available from September 1981 onward on a 1° by 1° resolution. ENSO evolution is described by the Niño3.4 index, which is defined as SST anomalies (SSTAs) averaged over 5°S–5°N, 170°W–120°W. Monthly means of outgoing long-wave radiations (OLR) on a 2.5° × 2.5° grid are from Liebmann and Smith (1996), which is used to represent deep convection variation associated with ENSO evolution. The surface wind stress is represented by pentad and monthly mean surface winds from NCEP/DOE reanalysis. The wind stress was calculated using the drag coefficient derived with a modified Charnock formula and empirical stability functions (Xue et al., 2011).

To assess hindcasts of the La Niña in 1998–2001 and real-time predictions of the La Niña in 2020–2023, we examine the predictions from six models in the North American Multimodel Ensemble project (NMME; Kirtman et al., 2014). The six models are NCEP CFSv2, the National Aeronautics and Space Administration NASA_GEOS5v2, the National Center for Atmospheric Research NCAR_CCSM4, the Geophysical Fluid Dynamics Laboratory GFDL_SPEAR, and the Environment and Climate Change Canada CanCM4i and GEM_NEMO. The predictions (hindcasts and real-time predictions) start from January 1982 to the present with a range of 9 months. However, due to the unavailability of some data in the 9-month lead time, in this work, we only examine the 1–8 months leads. The ensemble members range from 4 to 24 and the spatial resolution of the NMME data is 1° × 1°. Details about the models and data can be found in Kirtman et al. (2014) and https://www.cpc.ncep.noaa.gov/products/NMME/.

Except for the OIv2.1 SST starting from November 1981 and NMME from January 1982, all other observational-based data used in this work are from January 1979 onward. All the anomalies are computed as the departures from climatologies based on January 1991 to December 2020.

3. Evolution of the La Niñas During 2020–2023 and 1998–2001

For the 2020–2023 triple-dip La Niña event, the negative SSTAs emerged in the spring of 2020, and peaked in late 2020 and early 2021 (shading in Figure 2a). After the weakening in the spring and summer of 2021, the negative SSTAs restrengthened during late 2021 and early 2022. The negative SSTAs mostly persisted into spring 2022, lasted until the following winter, then gradually declined and returned to neutral conditions in February 2023. This SSTA evolution (shading in Figure 2a) was coherent with the fluctuations in both surface wind stress (vectors in Figure 2b) and deep convection anomalies (shading in Figure 2b). SSTA variations were also linked to wind-forced Kelvin wave activity along the equator (Figure 2a). For example, the initiation of negative SSTAs in the spring of 2020 occurred in response to an upwelling Kelvin wave and reduction of negative SSTAs during early and late 2021 were caused by two downwelling Kelvin waves. The small fluctuations in SSTA and the

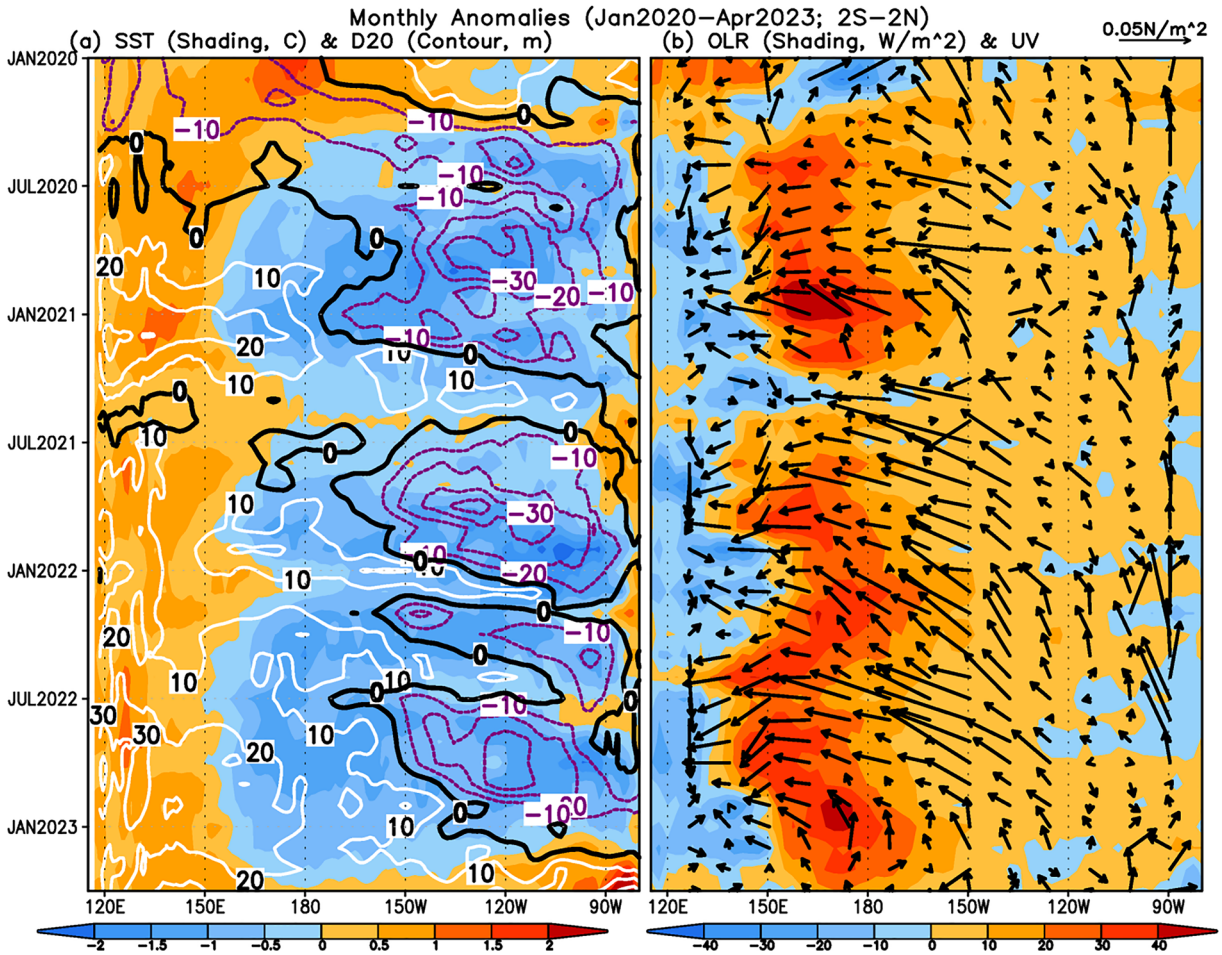

Figure 2. Hovmöller diagrams of the monthly mean of (a) sea surface temperature (SST) (shading) and D20 (contours), and (b) outgoing long-wave radiations (OLR) (shading) and surface wind stress (vector) anomalies averaged in 2°S–2°N during January 2020 to April 2023. The units are °C for SST, m for D20, W/m^2 for OLR, and N/m^2 for wind stress. The contours in white, black, and purple in (a) represent positive, zero, and negative D20 anomalies, respectively.

Niño3.4 index during October 2021 to December 2022 were also consistent with multiple weak upwelling and downwelling Kelvin waves.

For the triple-dip La Niña event in 1998–2001, the negative SSTAs were initiated in the spring of 1998 after the decay of the extremely strong El Niño in 1997–1998 (Figures 1b and 3a; see also McPhaden, 1999). The negative SSTAs peaked in late 1998, weakened during the spring and summer of 1999, and restrengthened in the fall of 1999 and the winter of 1999–2000. After weakening during the spring and summer of 2000, negative SSTAs peaked again for a third time in the fall of 2000 and the winter of 2000–2001. However, this third peak was much weaker than the previous two. Negative SSTAs eventually disappeared in the summer of 2001 and conditions returned to normal. Both suppressed deep convection and surface easterly wind stress anomalies (Figure 3b) were largest during periods of peak negative SSTA during 1998–2001. Similar to the event in 2020–2023, the evolution of SSTAs in 1998–2001 was also linked to Kelvin wave activity though Kelvin waves are less evident in these monthly analyzed data than in higher resolution mooring time series data (e.g., McPhaden, 1999). In short, the evolution of the basin-wide atmospheric and oceanic anomalies during the triple-dip La Niñas of 1998–2001 and 2020–2023 was broadly consistent with coupled ocean-atmosphere interactions involving wind-SST-thermocline feedbacks that we expect to operate during ENSO events (Bjerknes, 1969; C. Wang, 2018).

However, the two triple-dip La Niñas showed considerable differences in their detailed structure and evolution. For example, the negative D20 anomalies along the equatorial Pacific were stronger and more persistent during 1998–2001 La Niña (Figure 3a) than during 2020–2023 La Niña (Figure 2a) consistent with the stronger oceanic heat discharge associated with the extremely strong El Niño in 1997–1998 (Figure 1). On the other hand, although

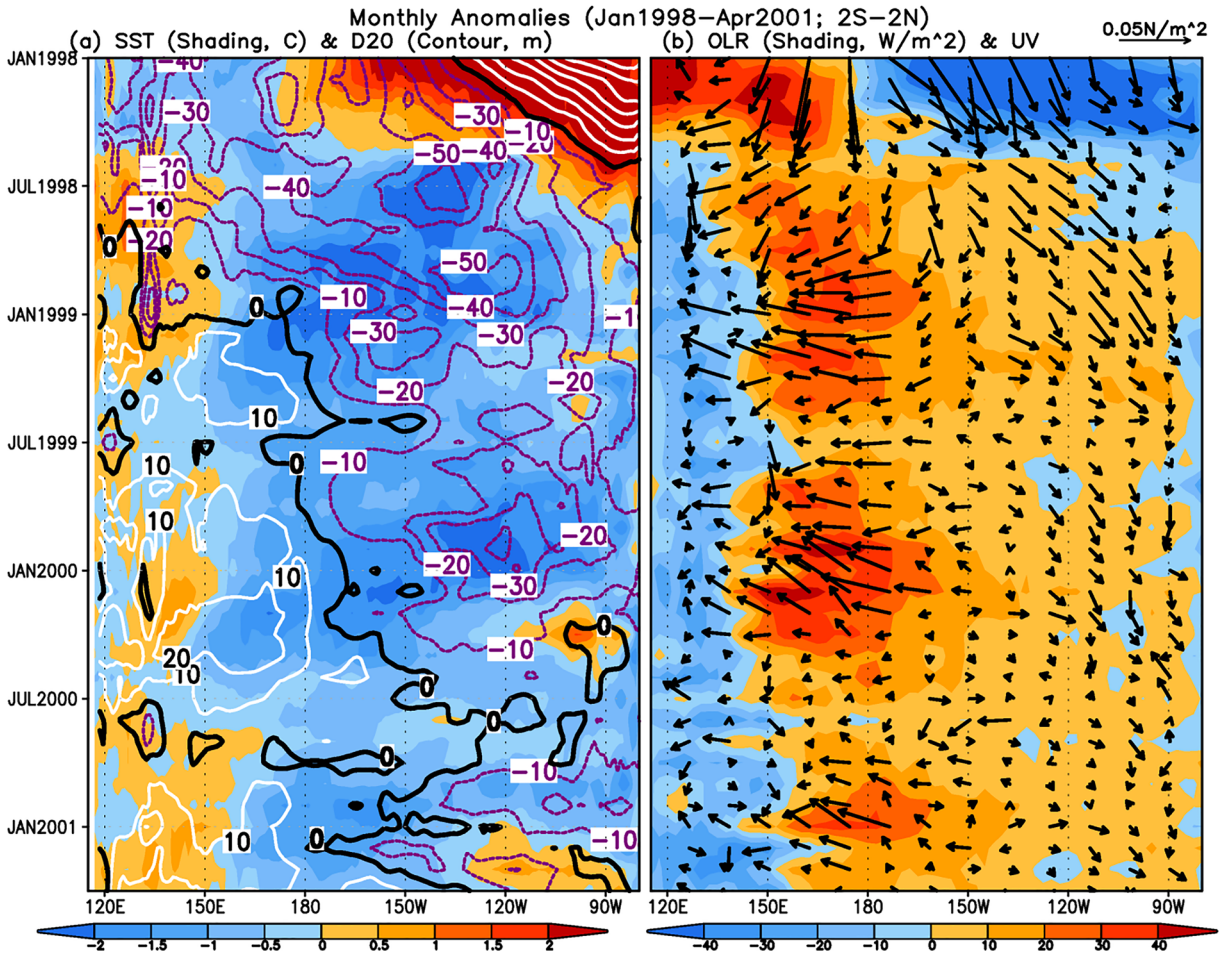

Figure 3. Hovmöller diagrams of the monthly mean of (a) sea surface temperature (SST) (shading) and D20 (contours), and (b) outgoing long-wave radiations (OLR) (shading) and surface wind stress (vector) anomalies averaged in 2°S–2°N during January 1998 to April 2001. The units are °C for SST, m for D20, W/m^2 for OLR, and N/m^2 for wind stress. The contours in white, black, and purple in (a) represent positive, zero, and negative D20 anomalies, respectively.

subsurface cooling (as represented by negative D20 anomalies) was weaker during the 2020–2023 La Niña, surface easterly wind anomalies were stronger and steadier (see pentad wind stress anomalies in Figure S3 in Supporting Information S1). These more persistent and stronger easterly wind anomalies during 2020–2023 were linked to the stronger warming in the western tropical Pacific (Figures 2 and 3).

4. Impact of the Mean State Changes in the Tropical Pacific

The differences between the two events were associated with mean state changes in the tropical Pacific which can be seen by comparing linear trends over January 1982 to December 2022 and the differences between average conditions in January 2020 to January 2023 and January 1998 to January 2001 (Figure 4). The patterns of the linear trends and differences are similar and exhibit a La Niña-like structure with strengthened zonal SST and D20 anomaly gradients, strengthened zonal trade winds, and suppressed deep convection in the central equatorial Pacific. The warming trends in the western tropical Pacific are likely due to human -induced warming (e.g., Jiang & Zhu, 2020; Leung et al., 2022; Weller et al., 2016). These trends and differences are also consistent with the ENSO regime shift and mean state changes across the equatorial Pacific in 1999/2000 (England et al., 2014; Z.-Z. Hu et al., 2013, 2020; Lee et al., 2022; Xiang et al., 2013; W. J. Zhang et al., 2010) though this shift was modulated by shorter time scale fluctuations (e.g., Capotondi & Qiu, 2023) and the major 2015–2016 El Niño (e.g., S. Hu & Fedorov, 2017; Li, Hu, & Huang, 2019; L'Heureux et al., 2017).

To examine the influence of the trends on the differences between the two La Niñas, we repeated the difference calculation in Figures 4c and 4d after linearly detrending the data (not shown). As expected, the zonal contrast

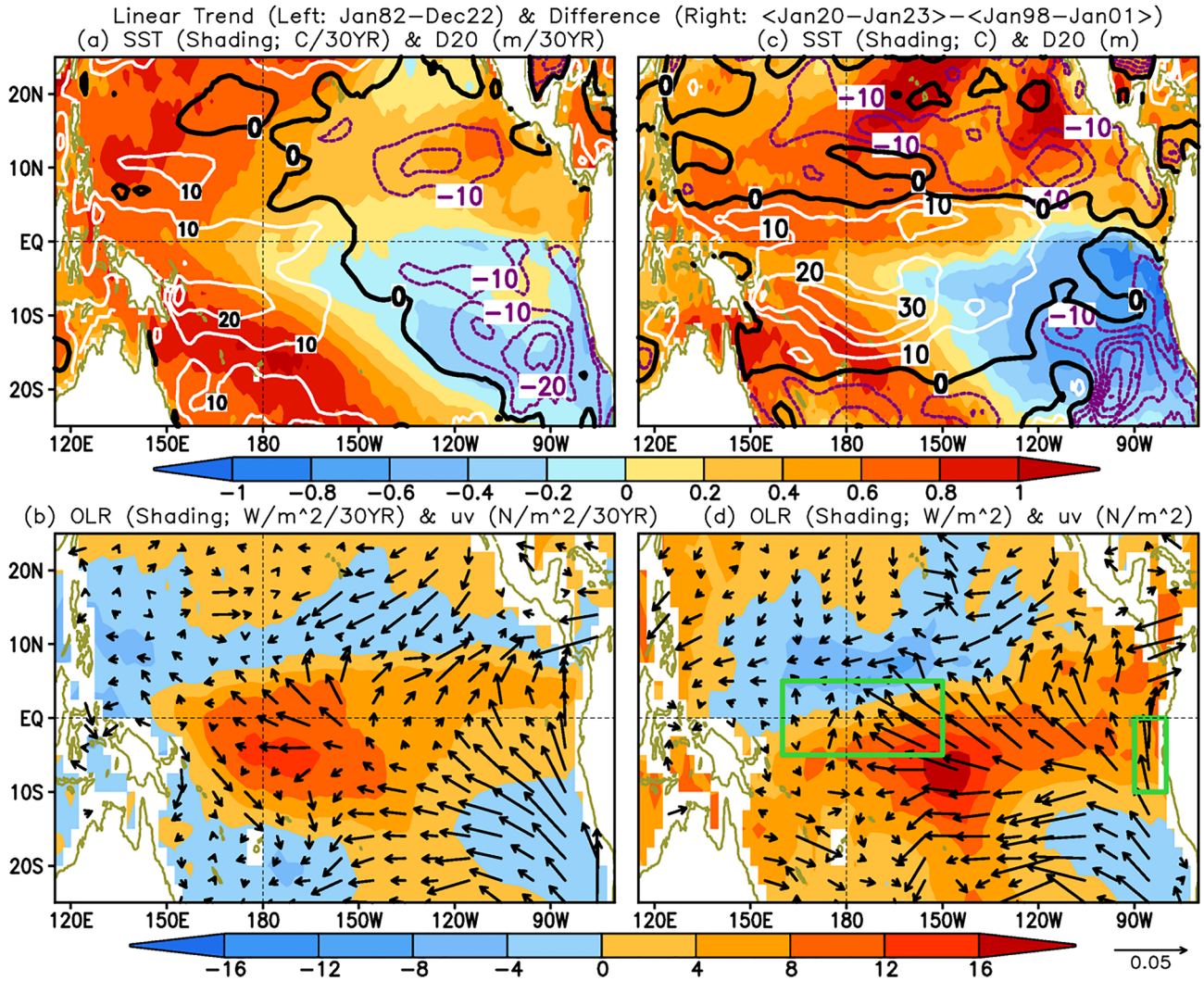

Figure 4. Anomalous linear trends of monthly means of (a) sea surface temperature (SST) (shading; °C/30 years) and D20 (contours; m/30 years), and (b) outgoing long-wave radiations (OLR) (shading; W/m^2/30 years) and surface wind stress (vectors; N/m^2/30 years) over land during January 1982 to December 2022. Anomalous differences between the monthly means in January 2020 to January 2023 and January 1998 to January 2001 for (c) SST (shading; °C) and D20 (contours; m), and (d) OLR (shading; W/m^2) and surface wind stress (vectors; N/m^2). The contours in white, black, and purple in (a), (c) represent positive, zero, and negative values, respectively. The green rectangles in (d) represent the Niño4 and Niño1+2 regions, respectively.

for both SST and D20 differences were reduced and the positive OLR difference in the eastern tropical Pacific decreased. However, the difference pattern was still evident implying an impact of the mean state change on the evolution of the 2020–2023 La Niña.

The mean state change and long-term trends were associated with a zonal SSTA gradient change across the tropical Pacific, which can be represented by Niño4-Niño1+2. The gradient was mostly negative in 1998–2001 La Niña (Figure 5a), which would not have favored persistent easterly wind anomalies (Lindzen & Nigam, 1987). In contrast, the gradient was mostly positive in 2020–2023 La Niña (Figure 5b), which would have favored persistent easterly wind anomalies. Thus, human -induced warming of the western Pacific warm pool and the strengthened zonal SST gradient likely contributed to the persistent easterly wind anomalies during the 2020–2023 triple-dip La Niña. Fang et al. (2023) also argued that the exceptionally strong southeasterly trade winds in March 2022 may have a key role in generating the third year of the 2022–2023 La Niña.

The differences in the mean state led to differences in the physical processes associated with the two triple-dip La Niñas (W. Wang & McPhaden, 2001). Specifically, for the Niño3.4 region (Figure 6), ocean vertical entrainment and diffusion (Q_w and Q_{zz}) were stronger during 1998–2001 than during 2020–2023, while zonal advection

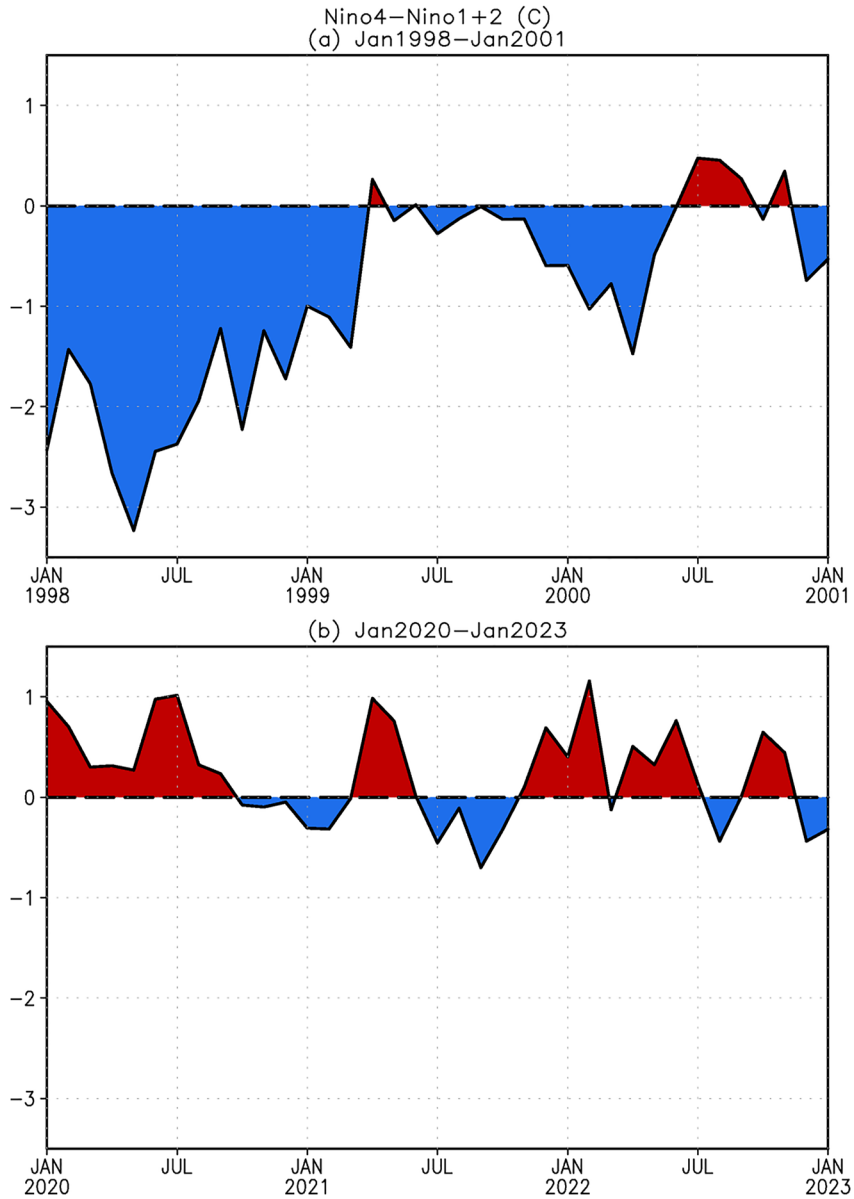

Figure 5. Zonal sea surface temperature anomaly gradient (Niño4-Niño1+2) during (a) January 1998 to January 2001 and (b) January 2020 to January 2023 (°C). The anomalies are referred to a 1991–2020 climatology.

was large and negative during 2020–2023 but positive during 1998–2001. In contrast, meridional advection and heat flux damping exhibited relatively small differences between the two triple-dip La Niñas. Thus, we hypothesize that the growth and maintenance of the triple-dip La Niña in 1998–2001 was mainly driven by ocean vertical entrainment and diffusion, as well as meridional advection, consistent with an enhanced equatorial upwelling circulation; while for the triple-dip La Niña in 2020–2023, zonal advection was the largest contributor followed by meridional advection and vertical entrainment and diffusion. The importance of the zonal advection in 2020–2023 was consistent with the stronger mean zonal SST gradient along the equator at that time as a result of the long-term trend. These results are also consistent with those of Lübbecke and McPhaden (2014) who showed from a Bjerknes stability index analysis that the mean state changes described here reduced the effectiveness of thermocline feedbacks in the eastern Pacific and resulted in a more stable ENSO cycle in the twenty-first century relative to the late twentieth century, which would favor the persistence of unusually cold conditions like those observed in 2020–2023. We next explore how these factors affected the predictability of the two events.

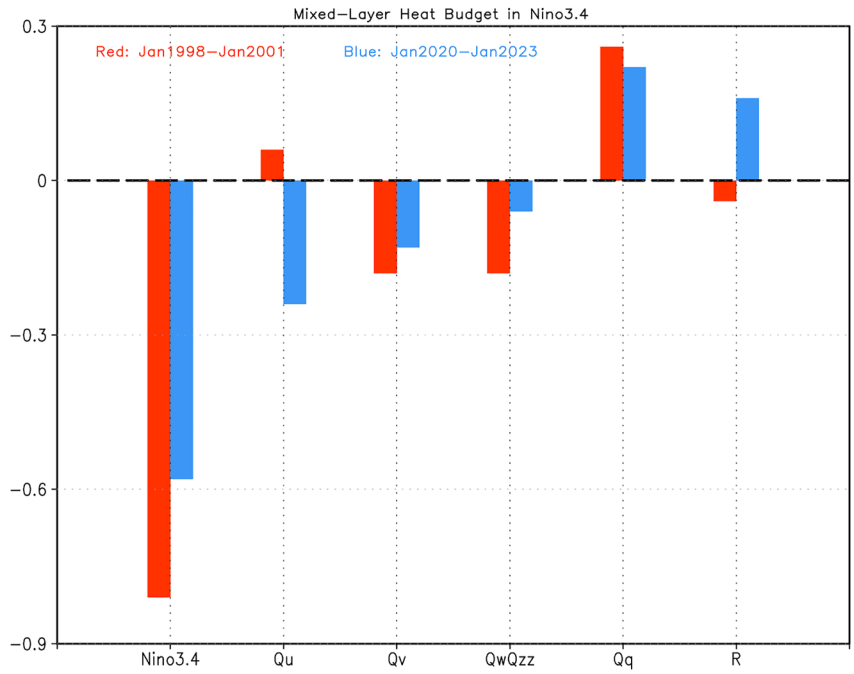

Figure 6. Niño3.4 region averaged pentad mean sea surface temperature (°C), Q_u, Q_v, $Q_w + Q_{zz}$, Q_q, and R (°C/month) during January 1998 to January 2001 (red bars) and January 2020 to January 2023 (blue bars). The anomalies are referred to a 1991–2020 climatology.

5. NMME Predictions

The real-time evolution of the 2020–2023 La Niña event was generally well predicted by both the ensemble of dynamical and statistical models collated by the International Research Institute for Climate and Society (IRI; https://iri.columbia.edu/our-expertise/climate/forecasts/enso/current/?enso_tab=enso-sst_table) and by NMME (https://www.cpc.ncep.noaa.gov/products/NMME/). Among the six NMME model predictions (Figure 7a, an example of 8-month lead predictions), NCEP CFSv2 was generally the best, while GFDL_SPEAR had appreciable warm biases and NASA_GEOS5v2 had obvious cold biases. Overall, for 1–8 months lead times, NMME (Figure S4a in Supporting Information S1) captured the evolution of the triple-dip La Niña during 2020–2023, especially the cooling in the second half of 2020 and 2021.

For the triple-dip La Niña in 1998–2001, the NMME hindcasts overestimated the amplitude of the first negative SSTA peak in the winter of 1998–1999, captured the second negative SSTA peak in the winter of 1999–2000, but failed to capture the third and minor negative SSTA peak in the winter of 2000–2001 (Figure 7b for 8-month lead and Figure S4b in Supporting Information S1 for 1–7 months leads). The failure of the model prediction during 2000–2001 might be due to the small SSTA, since a small signal (or equivalently low signal-to-noise ratio) is generally associated with low ENSO predictability (Z.-Z. Hu et al., 2019). Thus, the multi-model ensemble means from NMME captured the triple-dip La Niñas in 1998–2000 and 2020–2023 more than half a year in advance, but not the third negative peak in the boreal winter of 2000–2001.

The overall successful prediction of SSTA evolution during 2020–2023 (except for the timing of the third peak in the second half of 2022) may be linked to the prevailing mean state changes (Figure 4) involving persistent easterly wind anomalies and the strengthened zonal SSTA gradient, with a warmer western Pacific and cooler eastern Pacific. Figure 8 depicts the NMME averaged SSTA differences between the two triple-dip La Niña periods, which show that the averaged zonal SSTA gradient is larger in the triple-dip La Niña in 2020–2023 than that in 1998–2001 in the NMME predictions. Persistent and strongly coupled SSTs and winds would be incorporated into the initial conditions for the model predictions. Subsurface heat content precursors, which are generally considered a major source of predictability for ENSO, were small or unfavorable for this event (Figure 1). It is possible therefore that despite weak subsurface cooling, predictability for the 2020–2023 La Niña may have been boosted by the trends in background conditions. Thus, the prediction skill difference between the two triple-dip La Niñas may well have been associated with the mean state changes in the tropical Pacific.

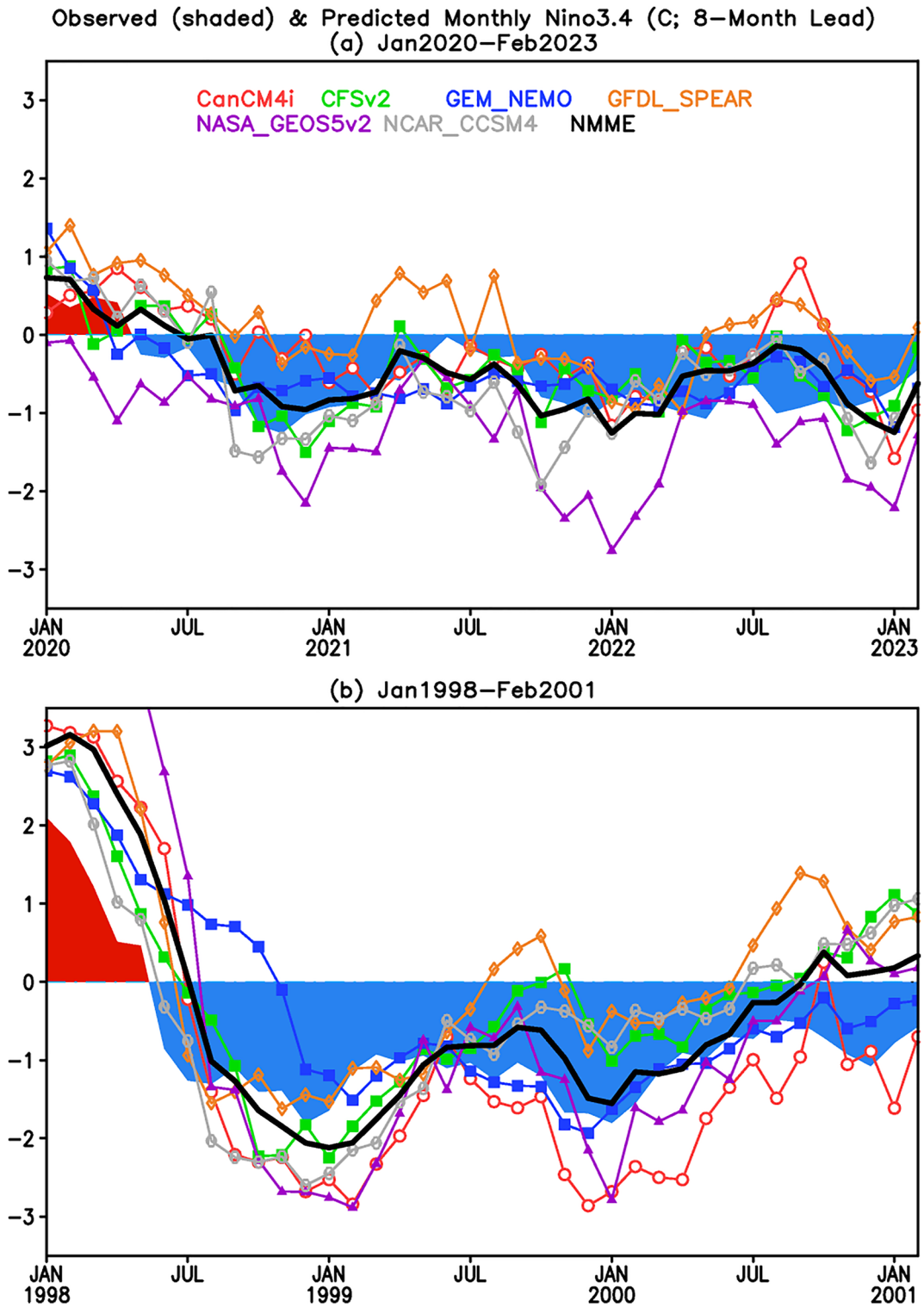

Figure 7. Observed (shading) and North American Multimodel Ensemble (NMME) six-models predicted monthly mean Niño3.4 index in (a) April 2020 to February 2023 and (b) April 1998 to February 2001. The curves represent the predictions with an 8-month lead of the six models and the black lines denote their mean. The unit is °C.

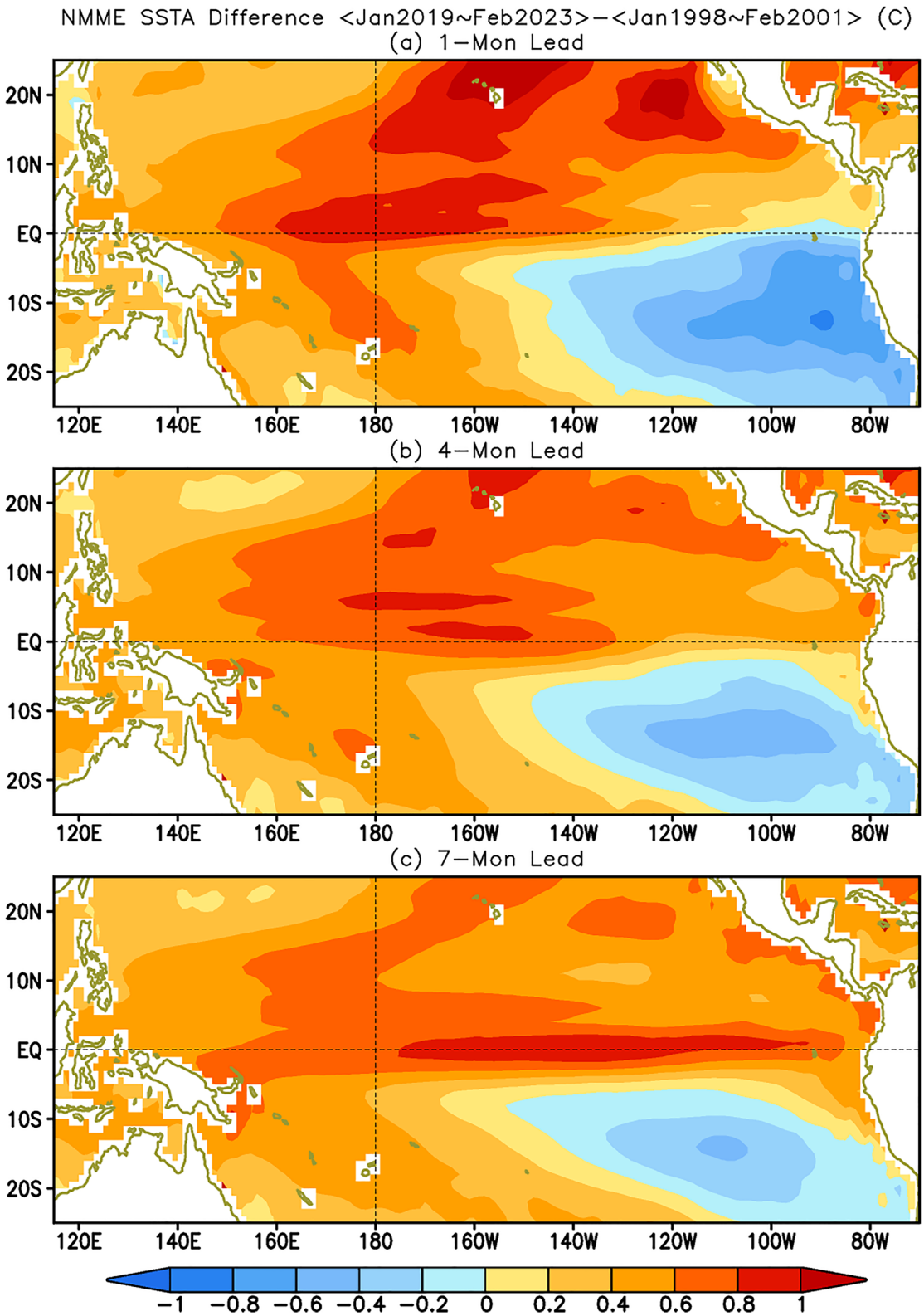

Figure 8. North American Multimodel Ensemble (NMME) averaged sea surface temperature anomaly (SSTA) differences between the means in January 2019 to February 2023 and January 1998 to February 2001 in (a) 1, (b) 4, and (c) 7-month leads. The unit is °C.

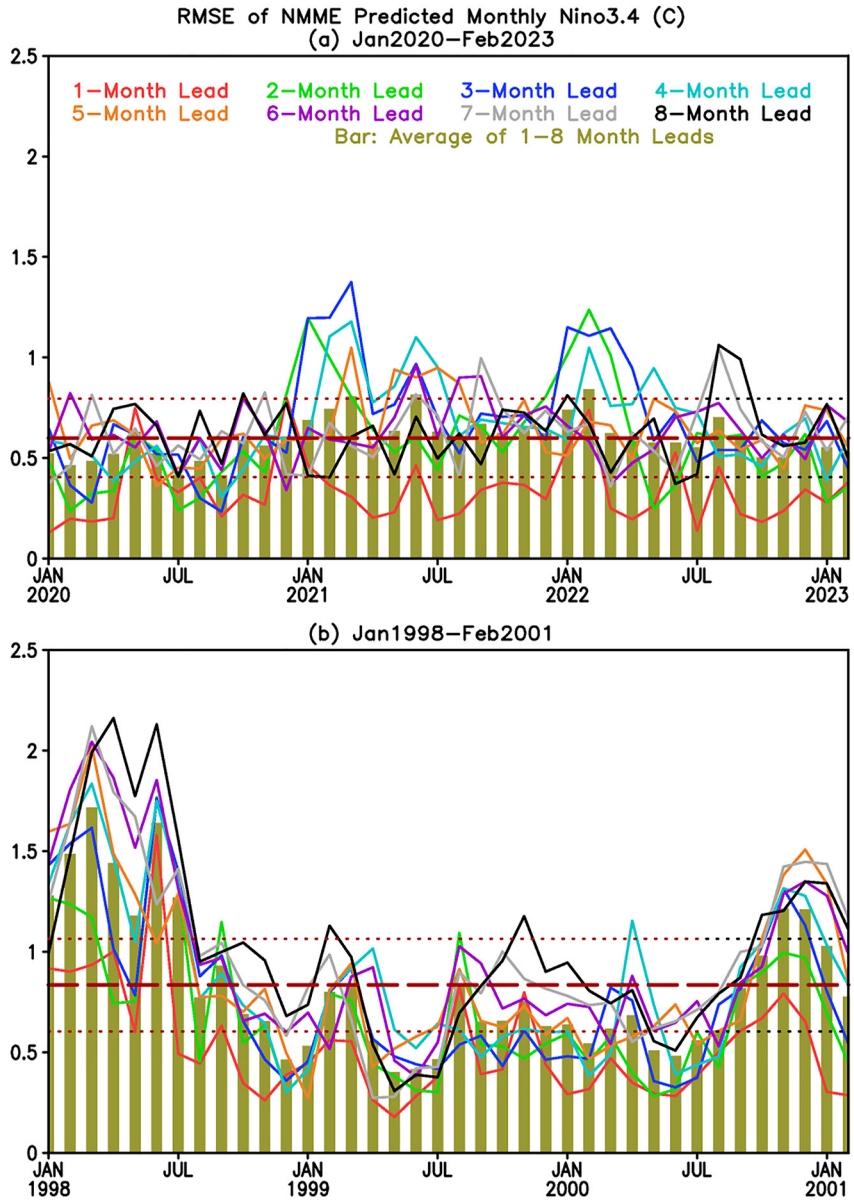

Figure 9. Root-Mean-Square-Errors (RMSE) of six models predicted monthly mean Niño3.4 index in (a) January 2020 to February 2023 and (b) January 1998 to February 2001 in 1–8 months leads. The bars are the average for 1–8 months leads. The unit is °C. Horizontal red dashed and dotted lines represent the mean RMSE of 1–8 leads and ±1 standard deviation over the 3 years of each prediction ensemble, respectively.

Mean state trends may also account for the relatively small fluctuations in the root-mean-square-errors (RMSE) for the 2020–2023 La Niña NMME predictions (Figure 9a), where RMSE is defined as the root mean square of the difference between the ensemble mean predicted Niño3.4 index for each model and observed Niño3.4 index. In contrast, RMSEs for 1998–2001 La Niña predictions were much more variable (Figure 9b), with large RMSE during initial phases in the first half of 1998 and the period of the third dip in late 2000. The triple-dip La Niña in 1998–2001 developed after the historically strong El Niño in 1997–1998 that was associated with a large discharge of upper ocean equatorial heat content (Figure 1b). Previous work has suggested that the magnitude of such a discharge is linked to the predictability of multi-year La Niñas, with a large discharge increasing the likelihood that La Niña conditions lasting more than 1 year would ensue (DiNezio et al., 2017; Wu et al., 2021). As a result, we might have expected that predictions initialized with a strong thermocline discharge or preceding major El Niño would show higher predictability than those with initial conditions of weaker magnitude. That proves

not to be the case in comparing these two triple-dip La Niñas, suggesting that mean state trends in the tropical Pacific over the past few decades may play a role in the predictability of the 2020–2023 La Niña. Indeed, we can see that the overall mean RMSE is slightly lower in 2020–2023 compared to 1998–2001, although the ranges of the RMSE fluctuation, measured by their standard deviation, are comparable (see the horizontal red dashed and dotted lines in Figure 9).

6. Summary and Discussion

Triple-dip La Niñas are a striking feature of ENSO evolution, representing a dramatic deviation from pure cyclic ENSO behavior. Here we compared the development and physical processes responsible for two triple-dip La Niña events in 1998–2001 and 2020–2023 in the context of mean state trends in the tropical Pacific. We also examined the prediction skill for the two events and discussed possible sources of predictability. The first event occurred in the wake of a strong El Niño in 1997–1998, while the second one occurred after a borderline El Niño in 2019–2020. Atmospheric and oceanic anomalies associated with the two triple-dip La Niñas exhibited considerable differences. The negative D20 anomalies in the equatorial Pacific were stronger and more persistent during 1998–2001 La Niña, due to the stronger oceanic heat discharge caused by the extreme 1997–1998 El Niño. In contrast, the surface easterly trade winds were stronger during the 2020–2023 La Niña, which can be linked to a mean state change in the equatorial Pacific Ocean SST zonal gradient. We propose that even without appreciable equatorial Pacific heat content discharge, persistent and strong surface easterly winds in balance with a stronger zonal SST contrast across the equatorial Pacific contributed to the development and predictability of the 2020–2023 triple-dip La Niña. In the absence of a significant subsurface precursor, the initial trigger for this event may have come from outside the Pacific basin through pan-tropical interactions (Cai et al., 2019; Hasan et al., 2022; Mukhopadhyay et al., 2022; C. Wang, 2019). This hypothesis does not rule out the possibility that influences from the extra-tropical north and south Pacific may also have contributed (Capotondi & Ricciardulli, 2021; Ding et al., 2022; Iwakiri & Watanabe, 2021; Park et al., 2021). For example, a North Pacific Oscillation–like variability is a possible source of multi-year El Niño events (Ding et al., 2022) and South Pacific Oscillation-like anomalies can affect the evolution of ENSO by modulating the southeasterly trade winds along the equatorial Pacific (You & Furtado, 2017). But once underway, strong positive Bjerknes feedbacks would have taken hold given the already favorably strong trade winds and east-west SST contrast.

The persistent warming in the western tropical Pacific favored the development of strong easterly wind anomalies in 2020–2023. This warming and increasing trade wind strength are likely related to the ENSO regime shift and the interdecadal variation of the mean state in the tropical Pacific since 2000 (Z.-Z. Hu et al., 2013, 2020; Xiang et al., 2013). The trend toward a more La Niña-like background state over the past 20 years would logically favor more frequent and longer lasting La Niñas just because of the shift toward colder mean conditions in the tropical Pacific, warmer mean conditions in the western basin, and stronger trade winds.

Some climate models suggest that greenhouse gas (GHG) forcing will result in a permanent La Niña-like mean state response (Kohyama et al., 2018; Watanabe et al., 2021). For example, GFDL Earth System Model Version 2M projected a La Niña-like mean state change with the ENSO amplitude decrease in a global warming scenario (Kohyama et al., 2018). The observed mean state change is thus potentially associated with global warming due to the increase in GHG concentrations in the atmosphere (Jiang & Zhu, 2018, 2020; Lee et al., 2022; and references therein). However, many more models suggest the opposite, namely that the response to GHG forcing is a permanent El Niño-like mean state (e.g., Cai et al., 2021). If that is the case, the observed strengthening of the easterlies and zonal SST gradient in the equatorial Pacific over the past few decades may be due to natural decadal variability associated with, for example, the Interdecadal Pacific Oscillation (e.g., Power et al., 2021). Regardless of the ultimate cause, the changing background conditions in the tropical Pacific appear to have significantly influenced the evolution and predictability of the 2020–2023 La Niña.

Seasonal NMME hindcasts and real-time predictions are limited to 8-month lead times. Thus, using this ensemble we cannot determine how predictable the 2020–2023 La Niña would have been at lead times longer than a year or how its predictability would have compared with the 1998–2001 La Niña at similar long lead times. Multi-year societally relevant climate prediction is emerging as a new area of research predicated in part on target phenomena like multi-year La Niñas for which there are various hypotheses to explain their evolution (https://usclivar.org/meetings/multi-year-workshop). The study can be viewed as a baseline contribution to those efforts that seek

to assess the longer lead time predictability of these two La Niña events using appropriately designed hindcast experiments.

Conflict of Interest

The authors declare no conflicts of interest relevant to this study.

Data Availability Statement

OIv2.1 monthly mean SST, GODAS monthly and pentad mean data, NCEP/DOE reanalyzed monthly mean surface wind, NOAA monthly mean OLR data, and NMME predicted monthly mean SSTs are available at Behringer and Xue (2004), Huang et al. (2021), Kanamitsu et al. (2002), Kirtman et al. (2014), and Liebmann and Smith (1996), respectively.

Acknowledgments
We appreciated the constructive comments and insightful suggestions from reviewers and Dr. Chidong Zhang. Li was supported by the National Natural Science Foundation of China (41930967). Zhu was supported by the National Natural Science Foundation of China (41830969). Liu was supported by the National Natural Science Foundations of China (42175056), and Jianghuai Meteorological Joint Project of Anhui Natural Science Foundation (2208085UQ10). The procedure of the heat budget calculation used in this work was developed by Dr. Boyin Huang and is maintained by Dr. C. Wen. PMEL contribution no. 5943.

References

An, S.-I., Tziperman, E., Okumura, Y. M., & Li, T. (2020). ENSO irregularity and asymmetry. In M. J. McPhaden, A. Santoso, & W. Cai (Eds.), *El Niño Southern Oscillation in a changing climate*. https://doi.org/10.1002/9781119548164.ch7

Behringer, D. W., & Xue, Y. (2004). Evaluation of the Global Ocean Data Assimilation System at NCEP: The Pacific Ocean [Dataset] Preprints. In *Eighth symp. on integrated observing and assimilation systems for atmosphere, oceans, and land surface*. Amer. Meteor. Soc. 2.3. Retrieved from http://ams.confex.com/ams/84Annual/techprogram/paper_70720.htm. https://www.esrl.noaa.gov/psd/data/gridded/data.godas.html

Bjerknes, J. (1969). Atmospheric teleconnections from the equatorial Pacific. *Monthly Weather Review*, *97*(3), 163–172. https://doi.org/10.1175/1520-0493(1969)097<0163:ATFTEP>2.3.CO;2

Cai, W., Santoso, A., Collins, M., Dewitte, B., Karamperidou, C., Kug, J. S., et al. (2021). Changing El Niño Southern Oscillation in a warming climate. *Nature Reviews Earth & Environment*, *2*(9), 628–644. https://doi.org/10.1038/s43017-021-00199-z

Cai, W., Wu, L., Lengaigne, M., Li, T., McGregor, S., Kug, J. S., et al. (2019). Pantropical climate interactions. *Science*, *363*(6430), 1–11. https://doi.org/10.1126/science.aav4236

Capotondi, A., & Qiu, B. (2023). Decadal variability of the pacific shallow overturning circulation and the role of local wind forcing. *Journal of Climate*, *36*(3), 1001–1015. https://doi.org/10.1175/JCLI-D-22-0408.1

Capotondi, A., & Ricciardulli, L. (2021). The influence of Pacific winds on ENSO diversity. *Scientific Reports*, *11*(1), 18672. https://doi.org/10.1038/s41598-021-97963-4

Capotondi, A., Wittenberg, A. T., Newman, M., Di Lorenzo, E., Yu, J. Y., Braconnot, P., et al. (2015). Understanding ENSO Diversity. *Bulletin America Meteorology Social*, *96*(6), 921–938. https://doi.org/10.1175/BAMS-D-13-00117.1

DiNezio, P. N., & Deser, C. (2014). Nonlinear controls on the persistence of La Niña. *Journal of Climate*, *27*(19), 7335–7355. https://doi.org/10.1175/jcli-d-14-00033.1

DiNezio, P. N., Deser, C., Okumura, Y., & Karspeck, A. (2017). Predictability of 2-year La Niña events in a coupled general circulation model. *Climate Dynamics*, *49*(11–12), 4237–4261. https://doi.org/10.1007/s00382-017-3575-3

Ding, R., Tseng, Y.-H., Di Lorenzo, E., Shi, L., Li, J., Yu, J.-Y., et al. (2022). Multi-year El Niño events tied to the North Pacific Oscillation. *Nature Communications*, *13*(1), 3871. https://doi.org/10.1038/s41467-022-31516-9

England, M. H., McGregor, S., Spence, P., Meehl, G. A., Timmermann, A., Cai, W., et al. (2014). Recent intensification of wind-driven circulation in the Pacific and the ongoing warming hiatus. *Nature Climate Change*, *4*(3), 22–227. https://doi.org/10.1038/nclimate2106

Fang, X., Zheng, F., Li, K., Hu, Z.-Z., Ren, H., Wu, J., et al. (2023). Will the history-record southeasterly wind in March 2022 trigger a third-year La Niña event? *Advances in Atmospheric Sciences*, *40*(1), 6–13. https://doi.org/10.1007/s00376-022-2147-6

Gao, C., Chen, M., Zhou, L., Feng, L., & Zhang, R.-H. (2022). The 2020-21 prolonged La Niña evolution in the tropical Pacific. *Science China Earth Sciences*, *65*(12), 2248–2266. https://doi.org/10.1007/s11430-022-9985-4

Gao, Z., Hu, Z.-Z., Zheng, F., Li, X., Li, S., & Zhang, B. (2023). Single-year and double-year El Niños. *Climate Dynamics*, *60*(7–8), 2235–2243. https://doi.org/10.1007/s00382-022-06425-8

Hasan, N. A., Chikamoto, Y., & McPhaden, M. J. (2022). The influence of tropical basin interactions on the 2020-2022 double-dip La Niña. *Frontiers in Climate*, *4*, 1001174. https://doi.org/10.3389/fclim.2022.1001174

Hayashi, M., & Jin, F.-F. (2017). Subsurface nonlinear dynamical heating and ENSO asymmetry. *Geophysical Research Letters*, *44*(24), 12427–12435. https://doi.org/10.1002/2017GL075771

Hu, S., & Fedorov, A. V. (2017). The extreme El Niño of 2015–2016 and the end of global warming hiatus. *Geophysical Research Letters*, *44*(8), 3816–3824. https://doi.org/10.1002/2017GL072908

Hu, Z.-Z., Kumar, A., & Huang, B. (2016). Spatial distribution and the interdecadal change of leading modes of heat budget of the mixed-layer in the tropical Pacific and the association with ENSO. *Climate Dynamics*, *46*(5–6), 1753–1768. https://doi.org/10.1007/s00382-015-2672-4

Hu, Z.-Z., Kumar, A., Huang, B., Zhu, J., L'Heureux, M., McPhaden, M. J., & Yu, J.-Y. (2020). The interdecadal shift of ENSO properties in 1999/2000: A review. *Journal of Climate*, *33*(11), 4441–4462. https://doi.org/10.1175/JCLI-D-19-0316.1

Hu, Z.-Z., Kumar, A., Huang, B., Zhu, J., Zhang, R.-H., & Jin, F.-F. (2017). Asymmetric evolution of El Niño and La Niña: The recharge/discharge processes and role of the off-equatorial sea surface height anomaly. *Climate Dynamics*, *49*(7–8), 2737–2748. https://doi.org/10.1007/s00382-016-3498-4

Hu, Z.-Z., Kumar, A., Ren, H.-L., Wang, H., L'Heureux, M., & Jin, F.-F. (2013). Weakened interannual variability in the tropical Pacific Ocean since 2000. *Journal of Climate*, *26*(8), 2601–2613. https://doi.org/10.1175/JCLI-D-12-00265.1

Hu, Z.-Z., Kumar, A., Xue, Y., & Jha, B. (2014). Why were some La Niñas followed by another La Niña? *Climate Dynamics*, *42*(3–4), 1029–1042. https://doi.org/10.1007/s00382-013-1917-3

Hu, Z.-Z., Kumar, A., Zhu, J., Peng, P., & Huang, B. (2019). On the challenge for ENSO cycle prediction: An example from NCEP Climate Forecast System version 2. *Journal of Climate*, *32*(1), 183–194. https://doi.org/10.1175/JCLI-D-18-0285.1

Hu, Z.-Z., Xue, Y., Huang, B., Kumar, A., Wen, C., Xie, P., et al. (2022). Global ocean monitoring and forecast at NOAA Climate Prediction Center: 15 Years of operations. *Bulletin America Meteorology Social*, *103*(12), E2701–E2718. https://doi.org/10.1175/BAMS-D-22-0056.1

Huang, B., Hu, Z.-Z., Kennedy, J. J., & Zhang, H.-M. (2022). Sea surface temperatures. [In "State of the Climate in 2021"]. *Bulletin America Meteorology Social*, *103*(8), S150–S153. https://doi.org/10.1175/BAMS-D-22-0072.1

Huang, B., Liu, C., Banzon, V., Freeman, E., Graham, G., Hankins, B., et al. (2021). Improvements of the Daily Optimum Interpolation Sea Surface Temperature (DOISST) version 2.1 [Dataset]. Journal of Climate, *34*(8), 2923–2939. https://doi.org/10.1175/JCLI-D-20-0166.1. Retrieved from https://www.ncei.noaa.gov/products/optimum-interpolation-sst

Huang, B., Shin, C.-S., Shukla, J., Marx, L., Balmaseda, M., Halder, S., et al. (2017). Reforecasting the ENSO events in the past fifty-seven years (1958-2014). *Journal of Climate*, *30*(19), 7669–7693. https://doi.org/10.1175/JCLI-D-16-0642.1

Huang, B., Xue, Y., Zhang, D., Kumar, A., & McPhaden, M. J. (2010). The NCEP GODAS ocean analysis of the tropical Pacific mixed layer heat budget on seasonal to interannual time scales. *Journal of Climate*, *23*(18), 4901–4925. https://doi.org/10.1175/2010JCLI3373.1

Iwakiri, T., & Watanabe, M. (2021). Mechanisms linking multi-year La Niña with preceding strong El Niño. *Scientific Reports*, *11*, 1–11. https://doi.org/10.1038/s41598-021-96056-6

Jiang, N., & Zhu, C. (2018). Asymmetric changes of ENSO diversity modulated by the cold tongue mode under recent global warming. *Geophysical Research Letters*, *45*(22), 12506–12513. https://doi.org/10.1029/2018GL079494

Jiang, N., & Zhu, C. (2020). Tropical Pacific cold tongue mode triggered by enhanced warm pool convection due to global warming. *Environmental Research Letters*, *15*(5), 054015. https://doi.org/10.1088/1748-9326/ab7d5e

Jin, F.-F. (1997). An equatorial ocean recharge paradigm for ENSO. Part I: Conceptual model. *Journal of the Atmospheric Sciences*, *54*(7), 811–829. https://doi.org/10.1175/1520-0469

Kanamitsu, M., Ebisuzaki, W., Woollen, J., Yang, S. K., Hnilo, J. J., Fiorino, M., & Potter, G. L. (2002). NCEP-DOE AMIP-II reanalysis (R-2) [Dataset]. Bulletin America Meteorology Social, *83*(11), 1631–1643. https://doi.org/10.1175/BAMS-83-11-1631. Retrieved from https://psl.noaa.gov/data/gridded/data.ncep.reanalysis2.html

Kessler, W. S. (2002). Is ENSO a cycle or a series of events? *Geophysical Research Letters*, *29*(23), 40-1–40-4. https://doi.org/10.1029/2002GL015924

Kim, J. W., & Yu, J. Y. (2022). Single- and multi-year ENSO events controlled by pantropical climate interactions. *npj Climate and Atmospheric Science*, *5*(1), 88. https://doi.org/10.1038/s41612-022-00305-y

Kirtman, B. P., Min, D., Infanti, J. M., Kinter, J. L., Paolino, D. A., Zhang, Q., et al. (2014). The North American Multimodel Ensemble: Phase-1 seasonal-to-interannual prediction; Phase-2 toward developing intraseasonal prediction [Dataset]. Bulletin America Meteorology Social, *95*(4), 585–601. https://doi.org/10.1175/bams-d-12-00050.1. Retrieved from https://www.earthsystemgrid.org/search.html?Project=NMME&q=&page=1&rpp=20

Kohyama, T., Hartmann, D. L., & Battisti, D. S. (2018). Weakening of nonlinear ENSO under global warming. *Geophysical Research Letters*, *45*(16), 8557–8567. https://doi.org/10.1029/2018GL079085

Lee, S., L'Heureux, M., Wittenberg, A. T., Seager, R., O'Gorman, P. A., & Johnson, N. C. (2022). On the future zonal contrasts of equatorial Pacific climate: Perspectives from observations, simulations, and theories. *npj Climate and Atmospheric Science*, *5*(1), 82. https://doi.org/10.1038/s41612-022-00301-2

Leung, J. C.-H., Zhang, B., Gan, Q., Wang, L., Qian, W., & Hu, Z.-Z. (2022). Differential expansion speeds of Indo-Pacific warm pool and deep convection favoring pool under greenhouse warming. *npj Climate and Atmospheric Science*, *5*(1), 97. https://doi.org/10.1038/s41612-022-00315-w

L'Heureux, M., Takahashi, K., Watkins, A. B., Barnston, A. G., Becker, E. J., Di Liberto, T. E., et al. (2017). Observing and predicting the 2015-16 El Niño. *Bulletin America Meteorology Social*, *98*(7), 1363–1382. https://doi.org/10.1175/BAMS-D-16-0009.1

Li, X., Hu, Z.-Z., Ding, R., & Liu, Y. (2023). Which ENSO Index best represents its global influences? *Climate Dynamics*, 1–15. https://doi.org/10.1007/s00382-023-06804-9

Li, X., Hu, Z.-Z., & Huang, B. (2019). Contributions of atmosphere-ocean interaction and low-frequency variation to intensity of strong El Niño events since 1979. *Journal of Climate*, *32*(5), 1381–1394. https://doi.org/10.1175/JCLI-D-18-0209.1

Li, X., Hu, Z.-Z., Liang, P., & Zhu, J. (2019). Contrastive influence of ENSO and PNA on variability and predictability of North American winter precipitation. *Journal of Climate*, *32*(19), 6271–6284. https://doi.org/10.1175/JCLI-D-19-0033.1

Li, X., Hu, Z.-Z., Tseng, Y.-H., Liu, Y., & Liang, P. (2022). A historical perspective of the La Niña Event in 2020/21. *Journal of Geophysical Research: Atmospheres*, *127*(7), e2021JD035546. https://doi.org/10.1029/2021JD035546

Liebmann, B., & Smith, C. A. (1996). Description of a complete (interpolated) outgoing long wave radiation dataset [Dataset]. Bulletin America Meteorology Social, *77*, 1275–1277. https://doi.org/10.1175/1520-0477-77.6.1274. Retrieved from https://psl.noaa.gov/data/gridded/data.interp_OLR.html

Lindzen, R. S., & Nigam, S. (1987). On the role of sea surface temperature gradients in forcing low-level winds and convergence in the tropics. *Journal of the Atmospheric Sciences*, *44*(17), 2440–2458. https://doi.org/10.1175/1520-0469(1987)044<2418:OTROSS>2.0.CO;2

Lübbecke, J. F., & McPhaden, M. J. (2014). Assessing the 21st century shift in ENSO variability in terms of the Bjerknes stability index. *Journal of Climate*, *27*(7), 2577–2587. https://doi.org/10.1175/JCLI-D-13-00438.1

McPhaden, M. J. (1999). Genesis and evolution of the 1997-98 El Niño. *Science*, *283*(5404), 950–954. https://doi.org/10.1126/science.283.5404.950

McPhaden, M. J. (2023). The 2020-23 triple-dip La Niña. [In "State of the Climate in 2022"]. *Bulletin America Meteorology Social*, *85*(5), 677–696. (in press). https://doi.org/10.1175/bams-85-5-677

McPhaden, M. J., Santoso, A., & Cai, W. (2020). El Niño Southern Oscillation in a Changing Climate. *Geophysical Monograph*, *253*, 1–506. https://doi.org/10.1002/9781119548164

McPhaden, M. J., Timmermann, A., Widlansky, M. J., Balmaseda, M. A., & Stockdale, T. N. (2015). The curious case of the El Niño that never happened: A perspective from 40 years of progress in climate research and forecasting. *Bulletin America Meteorology Social*, *96*(10), 1647–1665. https://doi.org/10.1175/BAMS-D-14-00089.1

Meinen, C. S., & McPhaden, M. J. (2000). Observations of warm water volume changes in the equatorial Pacific and their relationship to El Niño and La Niña. *Journal of Climate*, *13*(20), 3551–3559. https://doi.org/10.1175/1520-0442(2000)013<3551:OOWWVC>2.0.CO;2

Mukhopadhyay, S., Gnanaseelan, C., Chowdary, J. S., Parekh, A., & Mohapatra, S. (2022). Pro-longed La Niña events and the associated heat distribution in the tropical Indian Ocean. *Climate Dynamics*, *58*(9–10), 2351–2369. https://doi.org/10.1007/s00382-021-06005-2

National Research Council. (2010). *Assessment of intraseasonal to interannual climate prediction and predictability* (p. 192). The National Academies Press. ISBN-10: 0-309-15183-X.

Ohba, M., & Ueda, H. (2009). Role of nonlinear atmospheric response to SST on the asymmetric transition process of ENSO. *Journal of Climate*, *22*(1), 177–192. https://doi.org/10.1175/2008jcli2334.1

Okumura, Y. M., Ohba, M., Deser, C., & Ueda, H. (2011). A proposed mechanism for the asymmetric duration of El Niño and La Niña. *Journal of Climate*, *24*(15), 3822–3829. https://doi.org/10.1175/2011JCLI3999.1

O'Lenic, E. A., Unger, D. A., Halpert, M. S., & Pelman, K. S. (2008). Developments in operational long-range climate prediction at CPC. *Weather and Forecasting*, *23*(3), 496–515. https://doi.org/10.1175/2007WAF2007042.1

Park, J.-H., An, S.-I., Kug, J.-S., Yang, Y.-M., Li, T., & Jo, J.-S. (2021). Mid-latitude leading double-dip La Niña. *International Journal of Climatology*, *41*(S1), E1353–E1370. https://doi.org/10.1002/joc.6772

Peng, P., Barnston, A. G., & Kumar, A. (2013). A comparison of skill between two versions of the NCEP Climate Forecast System (CFS) and CPC's operational short-Lead seasonal outlooks. *Weather and Forecasting*, *28*(2), 445–462. https://doi.org/10.1175/WAF-D-12-00057.1

Power, S., Lengaigne, M., Capotondi, A., Khodri, M., Vialard, J., Jebri, B., et al. (2021). Decadal climate variability in the tropical Pacific: Characteristics, causes, predictability and prospects. *Science*, *374*(6563), eaay9165. https://doi.org/10.1126/science.aay9165

Song, C., Zhang, X., Zheng, F., Chen, X., & Jiang, H. (2022). The roles of off-equatorial subsurface cold-water incursions in triggering the second-year cooling of the La Niña Event in 2021. *Journal of Marine Science and Engineering*, *10*(11), 1667. https://doi.org/10.3390/jmse10111667

Timmermann, A., An, S. I., Kug, J. S., Jin, F. F., Cai, W., Capotondi, A., et al. (2018). El Niño-Southern Oscillation complexity. *Nature*, *559*(7715), 535–545. https://doi.org/10.1038/s41586-018-0252-6

Wang, C. (2018). A review of ENSO theories. *National Science Review*, *5*(6), 813–825. https://doi.org/10.1093/nsr/nwy104

Wang, C. (2019). Three-ocean interactions and climate variability: A review and perspective. *Climate Dynamics*, *53*(7–8), 5119–5136. https://doi.org/10.1007/s00382-019-04930-x

Wang, W., & McPhaden, M. J. (2001). Surface layer temperature balance in the equatorial Pacific during the 1997–98 El Niño and 1998–99 La Niña. *Journal of Climate*, *14*(16), 3393–3407. https://doi.org/10.1175/1520-0442(2001)014<3393:sltbit>2.0.co;2

Watanabe, M., Dufresne, J.-L., Kosaka, Y., Mauritsen, T., & Tatebe, H. (2021). Enhanced warming constrained by past trends in equatorial Pacific sea surface temperature gradient. *Nature Climate Change*, *11*(1), 33–37. https://doi.org/10.1038/s41558-020-00933-3

Weller, E., Min, S.-K., Cai, W., Zwiers, F. W., Kim, Y.-H., & Lee, D. (2016). Human-caused Indo-Pacific warm pool expansion. *Science Advances*, *2*(7), e1501719. https://doi.org/10.1126/sciadv.1501719

Wu, X., Okumura, K., Deser, C., & Dinezio, P. (2021). Two-year dynamical predictions of ENSO event duration during 1954-2015. *Journal of Climate*, *34*(10), 1–50. https://doi.org/10.1175/JCLI-D-20-0619.1

Xiang, B., Wang, B., & Li, T. (2013). A new paradigm for the predominance of standing Central Pacific warming after the late 1990s. *Climate Dynamics*, *41*(2), 327–340. https://doi.org/10.1007/s00382-012-1427-8

Xue, Y., Huang, B., Hu, Z.-Z., Kumar, A., Wen, C., Behringer, D., & Nadiga, S. (2011). An assessment of oceanic variability in the NCEP Climate Forecast System reanalysis. *Climate Dynamics*, *37*(11–12), 2511–2539. https://doi.org/10.1007/s00382-010-0954-4

You, Y., & Furtado, J. C. (2017). The role of South Pacific atmospheric variability in the development of different types of ENSO. *Geophysical Research Letters*, *44*(14), 7438–7446. https://doi.org/10.1002/2017GL073475

Yu, J.-Y., & Fang, S.-W. (2018). The distinct contributions of the seasonal footprinting and charged-discharged mechanisms to ENSO complexity. *Geophysical Research Letters*, *45*(13), 6611–6618. https://doi.org/10.1029/2018gl077664

Yulaeva, E., & Wallace, J. M. (1994). The signature of ENSO in global temperature and precipitation fields derived from the microwave sounding unit. *Journal of Climate*, *7*(11), 1719–1736. https://doi.org/10.1175/1520-0442(1994)007<1719:TSOEIG>2.0.CO;2

Zhang, R.-H., Gao, C., & Feng, L. (2022). Recent ENSO evolution and its real-time prediction challenges. *National Science Review*, *9*(4), nwac052. https://doi.org/10.1093/nsr/nwac052

Zhang, R.-H., Zheng, F., Zhu, J., & Wang, Z. G. (2013). A successful real-time forecast of the 2010-11 La Niña event. *Scientific Reports*, *3*(1), 1108. https://doi.org/10.1038/srep01108

Zhang, W. J., Li, J. P., & Zhao, X. (2010). Sea surface temperature cooling mode in the Pacific cold tongue. *Journal of Geophysical Research*, *115*(C12), C12042. https://doi.org/10.1029/2010JC006501

Zhu, J., Kumar, A., Huang, B., Balmaseda, M. A., Hu, Z.-Z., Marx, L., & Kinter, J. L., III. (2016). The role of off-equatorial surface temperature anomalies in the 2014 El Niño prediction. *Scientific Reports*, *6*(1), 19677. https://doi.org/10.1038/srep19677